Friction ISSN 2223-7690
https://doi.org/10.1007/s40544-023-0827-6 CN 10-1237/TH
RESEARCH ARTICLE

High temperature lubrication performance of chlorophenyl silicone oil

Yan MENG[1,2], Xiangli WEN[2], Jie CHENG[1,*], Pengpeng BAI[2], Yonggang MENG[2], Yu TIAN[2,*]
[1] *School of Mechanical and Electrical Engineering, China University of Mining and Technology-Beijing, Beijing 100083, China*
[2] *Department of Mechanical Engineering, State Key Laboratory of Tribology in Advanced Equipment, Tsinghua University, Beijing 100084, China*
Received: 25 July 2022 / Revised: 14 October 2022 / Accepted: 19 September 2023

Abstract: Most studies of liquid lubricants were carried out at temperatures below 200 °C. However, the service temperature of lubricants for aerospace and aeroengine has reached above 300 °C. In order to investigate the friction mechanism and provide data for high temperature lubrication, the friction and wear properties of chlorophenyl silicone oil (CPSO)-lubricated M50 steel and Si_3N_4 friction pairs were investigated herein. Ball-on-disk experimental results show that the lubrication performance of CPSO varies significantly with temperature. Below 150 °C, coefficient of friction (COF) remains at 0.13–0.15 after the short running-in stage (600 s), while the COF in the running-in stage is 0.2–0.3. At 200 °C and above, the running-in time is much longer (1,200 s), and the initial instantaneous maximum COF can reach 0.5. Under this condition, the COF gradually decreases and finally stabilizes at around 0.16–0.17 afterwards. This phenomenon is mainly due to the different thickness of boundary adsorption film. More importantly, the wear rate of M50 steel increases significantly with the temperature, while the wear rate barely changes at temperatures above 200 °C. The anti-wear mechanism is explained as tribochemical reactions are more likely to occur between CPSO and steel surface with the increased temperature, generating the $FeCl_2$ protective film on the metal surface. Accordingly, $FeCl_2$ tribochemical film improves the lubrication and anti-wear capacity of the system. At high temperatures (200–350 °C), $FeCl_2$ film becomes thicker, and the contact region pressure becomes lower due to the larger wear scar size, so the wear rate growth of M50 steel is much smaller compared with that of low temperatures (22–150 °C). The main findings in this study demonstrate that CPSO lubricant has good anti-wear and lubrication capacity, which is capable of working under temperatures up to 350 °C.

Keywords: chlorophenyl silicone oil (CPSO); liquid lubricant; anti-wear; high temperature

1 Introduction

Extreme working conditions such as high temperature, high speed, low vacuum, and high load are more likely to cause lubrication failure of the working interface, resulting in abnormal wear and even equipment failure [1]. These problems will significantly impact the reliability and lifespan of the transmission system and the entire machine. The key to address these issues lies in developing a high-temperature-resistant lubricant and friction subsystem, which is the core technology required to solve these problems.

As a key moving part, the friction and wear of ball bearing at high temperatures especially above 300 °C are very important. From the point of view of friction pairs material, superalloy steel and ceramic fittings are used under high-temperature environments in the latest design. M50 as second-generation bearing steel has been used in the high-temperature field. M50 steel can maintain a hardness of over 60 HRC

* Corresponding authors: Yu TIAN, E-mail: tianyu@mail.tsinghua.edu.cn; Jie CHENG, E-mail: jiecheng@cumtb.edu.cn

at temperature below 315 °C [2]. Its anti-fatigue and anti-wear properties can be effectively enhanced by surface shot peening, ion implantation, et al. [3, 4]. In addition, Si_3N_4 ceramics have been widely used in the rolling elements of high-temperature bearings in the advanced industry due to their high strength & hardness, low density & expansion coefficient, as well as anti-oxidation, anti-corrosion and anti-abrasion properties at high temperature [5]. All-ceramic Si_3N_4 balls or roller bearings (with silicon nitride rolling elements and rings) can operate at high temperatures. But for most applications, hybrid ceramic silicon nitride bearings can meet the demands imposed by very high-speed, high-temperature operation. The main advantage of ceramic balls is to reduce the centrifugal loading on the outer raceway of the bearing, by the lower density (3.1 g/cm^3) compared to steel balls (8 g/cm^3). This also reduces the variation of contact angle between inner and outer raceways and, thereby, the sliding which causes an increase in bearing operating temperature and wear of bearing elements [6]. However, subject to the bearing temperature of lubricants, the friction and wear properties of the Si_3N_4 and M50 bearing steel under high temperature (above 300 °C) lubricated by oil have not yet been systematically carried out.

Most of the lubricants withstanding temperatures above 300 °C are synthetic new materials, mainly including modified silicone oil, perfluoropolyether (PFPE), fluoroether triazine, ionic liquid, and liquid metal [7]. All these new materials have thermal resistance properties. They are all outstanding but have particularities or defects, which limit their application in the field of lubrication to some specific occasions. PFPE has poor boundary lubrication performance. It is easily degraded and corrosive to metals, so it is mainly used in short-term service conditions [8]. Fluoroether triazine is easy to evaporate and has relatively poor fluidity at low temperatures [9]. Ionic liquids are corrosive to friction pairs, which limits their application in the field of tribology [10]. Gallium-based liquid metal is extremely sensitive to oxygen and reacts with most metals at high temperature [11–13]. The service temperature of modified silicone oil such as phenyl silicone oil can reach up to 300 °C [14], but its boundary lubrication ability is poor. Most modified silicone oils were used as aerospace instrument lubricants, such as turbine engine lubricants and bearing lubricants [15–17].

Modified silicone oil by adding specific groups shows improved lubricity [18, 19]. Schiefer et al. [20, 21] extend the utility of silicone lubricants through structural modifications. These modifications have increased the oxidation, thermal, and radiation resistance by high phenyl substitution. Likewise, the boundary lubricity and solvent resistance could be increased by fluoroalkyl substitution. Weng et al. [22] found that the chlorophenyl silicone oil (CPSO) and trifluorinated-propyl with methyl terminated silicone oil (FCPSO) show good tribological behavior for the steel/CuSn alloy tribological pairs. Results indicated the formation of $FeCl_2$ and FeF_2 during the sliding process, which prevents further wear and reduces friction. Jiang et al. [23] modified fluorosilicone oil by introducing chlorine atoms into the side chain of fluorosilicone oil to improve its lubricating performance. The Cl-containing fluorosilicone oil has good extreme pressure performance, excellent high-temperature oxidation stability and is non-corrosive to metals. Lv et al. [24] investigated the tribological performance of CPSO and PFPE in high-vacuum and irradiation environments. CPSO solid-liquid lubricating materials after irradiation have lower COF increments compared with that of PFPE. This indicates that CPSO has great potential in the field of high-temperature lubrication.

However, the lubrication performance and mechanism of CPSO at high temperatures (above 300 °C) are not clear. Most studies focus on steel-to-steel friction pairs using chlorophenyl silicone oil as lubricants under vacuum conditions or at temperatures below 100 °C. Therefore, the investigations of CPSO on ceramic-to-steel lubrication at high temperatures are still rare and are in urgent need, the results of which could provide theoretical and data support for the next generation of high-temperature bearings and lubricating materials. This paper, for the first time, uses CPSO, Si_3N_4 ceramic balls, and M50 steel to build high-temperature lubrication and friction pairs system to study the high-temperature lubrication behavior at temperatures up to 350 °C. The tribological characteristics, lubrication and anti-wear mechanism of such a system has been revealed. Results in this paper provide a theoretical basis and data support for the high-temperature lubricant and ceramic-to-steel friction pairs system.

2 Experimental

CPSO was commercially available from the Great Wall Lubricant Corporation of China. Si_3N_4 ball and M50 steel were purchased from. Sinoma Advanced Nitride Ceramics Co., Ltd., China. All the organic solvents (ethanol, petroleum ether, acetone) used in this work are AR grade, purchased from Aladdin Scientific Corp., China. Ultra-pure water with a conductivity of 18.2 MΩ·cm and a total organic carbon of less than 2 ppb was used as the solvent water.

2.1 Tribological test

In order to explore the friction and wear and performance of CPSO lubricant under different temperatures, tribological tests were performed by using high-temperature reciprocating friction and wear tester (SRV-4, Optimal, Germany, ASTM D5707-19) to evaluate the friction and wear behavior in the sliding motion [25]. Tribology experiments were carried out on optimal SRV-4 as exemplified in Fig. 1(a). The upper Si_3N_4 ceramic ball (diameter, 10.3 mm; R_a = 3 nm) of the SRV-4 tester slides reciprocally against the lower stationary M50 steel discs (Φ24 mm × 7.88 mm, R_a = 13 nm). Before the test, all the M50 specimens were polished progressively to 1200# using sandpaper. All the tests were conducted at the frequency of 50 Hz with a corresponding stroke length of 1 mm and sliding time of 60 min under 30 N applied load (Hertz contact pressure 1.607 GPa). Before the friction and wear test, 100 μL of the lubricant was introduced to the ball–disc contact area. The experimental temperature ranges from 22 to 350 °C. All the parameters and coefficient of friction (COF) will be recorded automatically once the experiment is finished. All experiments were repeated at least three times to ensure the accuracy. The used CPSO of each test was collected for analysis after the experiment. M50 steel discs and Si_3N_4 ball were ultrasonically cleaned sequentially with petroleum ether, acetone, and ethanol for 5 min, respectively. They were dried and stored to analyze the surface morphology and composition of the wear scar afterwards.

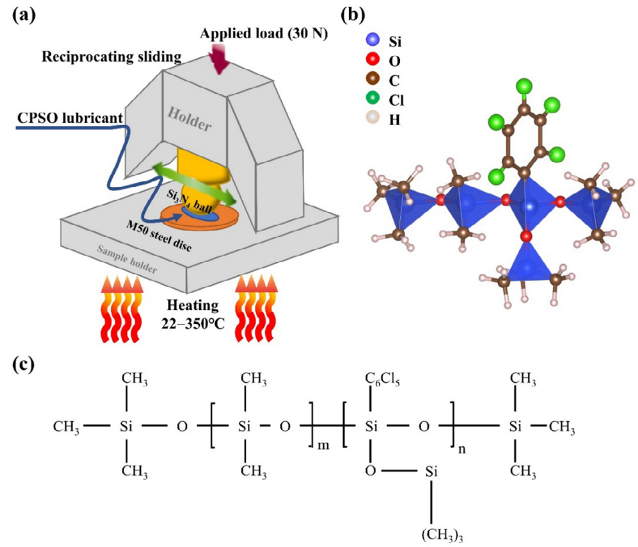

Fig. 1 (a) Schematic diagram of optimal SRV-4 and molecular structures of CPSO: (b) ball-and-stick model and (c) formula.

2.2 Characterization

The viscosity of CPSO at different temperatures was measured using a rheometer (MCR301, Aaton paar, Austria). The hardness of M50 steel at different temperatures was tested by an electromechanical hardness testing machine (ZONG-DE, China). The surrounding environment of high temperature hardness testing was filled with Ar (99.9% purity) as protective atmosphere. Both the oxygen content and water vapor content were maintained at 0.1 ppm in the glove box. With 5 °C/min heating rate and 1 kg stress force, 3 data were recorded at each testing temperature by calculating the diagonal length of square holes on the M50 surface. During the whole experiment, the pressure in the glove box was maintained at 120 Pa higher than the indoor pressure. The wear scar size (WSS) of Si_3N_4 balls and M50 steel discs were measured by an optical microscope (VHX600, Keyence, Japan) after each tribology test. The surface morphology of the wear scars on both M50 steel discs and Si_3N_4 ball and their wear volume loss were measured and calculated by the white light interferometer (New view 8300, Zygo, US). Fourier transform infrared spectra (FTIR, Nicolet ncxus 670, Madison, US) of CPSO before and after the tribological test were recorded in the range of 4,000–650 cm^{-1}. The micro-topography of the wear scars was observed using a scanning electron microscope (SEM, Quanta 200, FEI, US) equipped with energy-dispersive X-ray spectroscopy (EDS, Genesis xm-2, EDAX, US). X-ray photoelectron spectrometer (XPS, Quantera II, Ulvac-phi, US) analysis was carried out with Al-Ka radiation as the exciting source. XPS was used to identify the chemical composition of the wear scars during the sliding process.

3 Results and discussion

Figure 1 shows the molecular structure of CPSO. In the molecular structure of CPSO, a certain methyl group in the silicone oil molecule is replaced by a chlorophenyl group. The viscosity change of CPSO as a function of temperatures and the relationship between the viscosity logarithm and the reciprocal temperature of CPSO are shown in Fig. 2. The activation energy is calculated by the viscosity–temperature relationship fitted by the Arrhenius equation which is shown in Fig. 2. When the temperature increases from 22 to 150 °C, the viscosity of CPSO decreases by 87.54% (58.99 mPa·s). When the temperature is above 150 °C, the viscosity of CPSO is only 6.06 mPa·s. The silicon atom in the tetrahedron has a large atomic volume and the long bond length and large bond angle of Si–O–Si. The methyl group directly connected to it can rotate completely freely, which allows the change in viscosity with temperature [26]. Silicone oil can be spirally curled in the liquid state, which in turn unloads a large part of the intermolecular force, so the intermolecular force is very small [27]. The above regulates the viscosity changes of CPSO with temperature, so the change in viscosity will be much lower than that of other lubricating oils. The calculated viscosity flow activation energy is also higher than that of other liquid lubricants, which also proves that CPSO has better viscosity–temperature performance [28]. This characteristic viscosity will further affect the lubricating performance of CPSO hereinafter.

Figure 3 shows the hardness of M50 steel at different temperatures from 22 to 350 °C. As the temperature increases, the hardness of M50 steel drops by 7.15% which is consistent with the data described in the literature [29]. Although the hardness has decreased, it still maintains a high level above 60 HRC. Those indicate the M50 steel has big potential to show good anti-wear performance at high temperature. The Si_3N_4 ball could retain invariant high-level hardness (78 HRC) even at 1,000 °C [6].

3.1 Tribological performance

Figures 4(a) and 4(b) show the changes of COF between 22 and 350 °C. The COF in Fig. 4(c) shows distinct changes in the high-temperature range (above 150 °C) and the low-temperature range (below 150 °C). When the temperature is below 150 °C, after the initial running-in (600 s) period, the COF is stable at 0.13–0.15. When the temperature is above 150 °C, the running-in time is obviously longer (1,200 s), and the COF after running-in is unstable, gradually decreases, and finally stabilizes at 0.16–0.17. The running-in stage is mainly affected by the viscosity effect of boundary adsorption film. At the temperature is below 150 °C, CPSO molecules shrink into a spring state [26]. The boundary film is thick due to the relatively high viscosity. The wear between the friction pair is slight due to the boundary film being

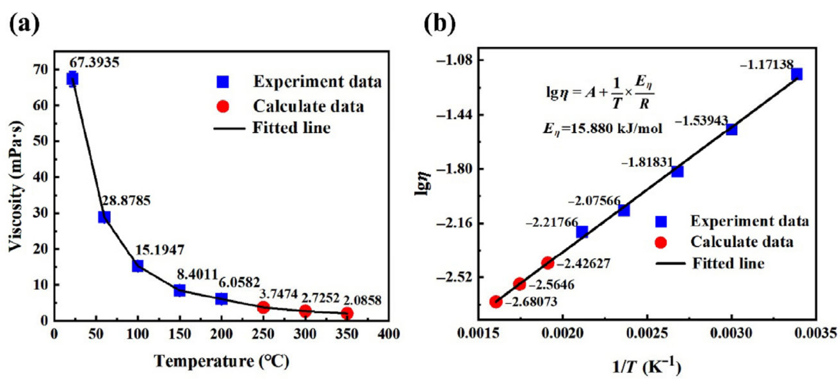

Fig. 2 (a) Viscosity results of CPSO at different temperatures and (b) the relationship between the viscosity logarithm and the reciprocal temperature of CPSO, η is the viscosity (Pa·s), A is the intercept constant, T is the temperature (K), R is the gas constant (kJ/(mol·K)), E_η is the activation energy (kJ/mol).

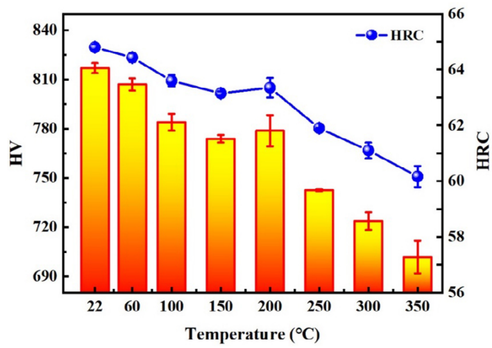

Fig. 3 Hardness of M50 steel at different temperatures.

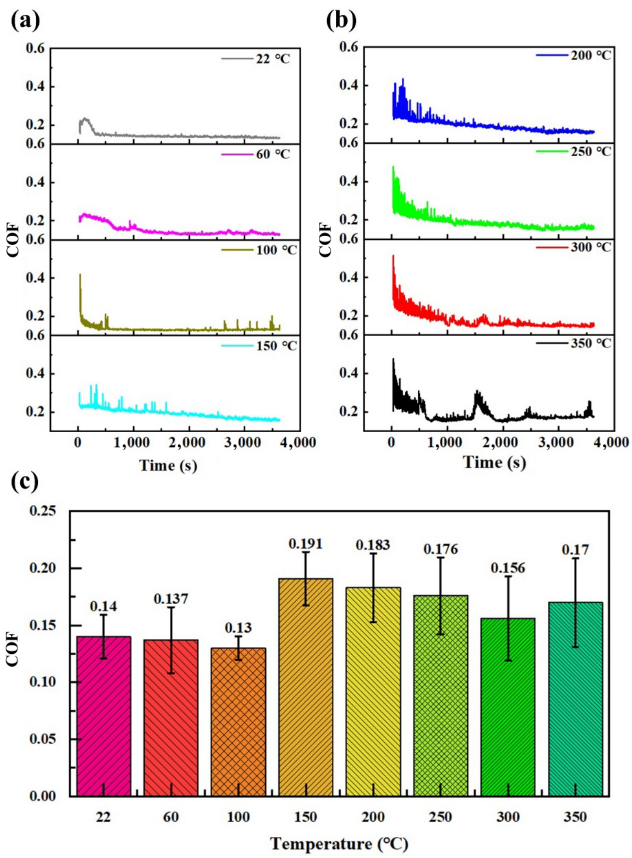

Fig. 4 (a) Frictional curves from 22 to 150 °C, (b) the frictional curves from 200 to 350 °C, and (c) COF at different temperatures.

thicker. As a result, it is easier and faster to obtain a uniform surface, which is the end of the running-in process [30, 31]. And when the temperature is above 150 °C, CPSO molecules are stretched, which makes the viscosity of CPSO decrease, to form a thinner boundary film. Combined with the severe wear, it is difficult to get a stable uniform surface. Therefore, the running-in period will be much longer due to the thinner film and severe wear [32].

Figure 5 shows the size of the wear scar by optical microscope. The WSS of M50 steel discs grows rapidly with temperature below 150 °C, but it remains slightly changed when the temperature is above 150 °C. Figure 6 shows the topography and depth profiles of wear scar at different temperatures. This can be also found in depth profiles shown in Figs. 6(b) and 6(c), that depth in the X direction and Y direction below 150 °C is less than 3 μm, which exceeds 6 μm when the temperature is above 150 °C.

The wear volume of balls and discs was measured by the white light interferometer. The calculated wear rate is shown in Fig. 7. It can be clearly seen that the wear rate of M50 disc has an inflection point at 150 °C. The wear rate increases by 954.9%, from 1.91×10^{-8} $mm^3/(N \cdot m)$ at 22 °C to 2.01×10^{-7} $mm^3/(N \cdot m)$ at 150 °C. But the increment of wear rate slows down at higher temperatures. It changes from 3.61×10^{-7} $mm^3/(N \cdot m)$ at 200 °C to 4.36×10^{-7} $mm^3/(N \cdot m)$ at 350 °C which increases by only 20.7%.

Figure 8 shows the topography of Si_3N_4 balls and X and Y depth profiles of wear scar at different temperatures. The depth in both X and Y direction increase with temperatures ranging from 22 to 250 °C. The depth of wear scar at 300 and 350 °C are smaller than that at 250 °C. The calculated wear rate of Si_3N_4 ball scars is shown in Fig. 9. It is obvious that under low-temperature conditions, the wear rate increases by 756.4%, from 1.10×10^{-8} $mm^3/(N \cdot m)$ at 22 °C to 8.32×10^{-8} $mm^3/(N \cdot m)$ at 150 °C. However, the wear rate significantly reduces by 29.5%, from 1.02×10^{-7} $mm^3/(N \cdot m)$ at 250 °C to 7.19×10^{-8} $mm^3/(N \cdot m)$ at 350 °C. The depth profiles of wear scar of Si_3N_4 ball shows similar variation tendency. The only difference between M50 steel disc and Si_3N_4 ball is the wear rate at high temperatures. The wear rate of Si_3N_4 ball at temperatures above 250 °C starts to decrease. This is because the service temperature of M50 steel discs is 315 °C, while the hardness of Si_3N_4 ceramic remains stable at temperatures up to 1,000 °C. The slight plastic deformation of steel would be helpful to the formation of larger WSS on M50 discs. However, the effect of plastic deformation of steel on wear rate due to thermal softening of M50 steel as well as oxidation of steel at high temperatures is insignificant, which can be seen in the reference [33].

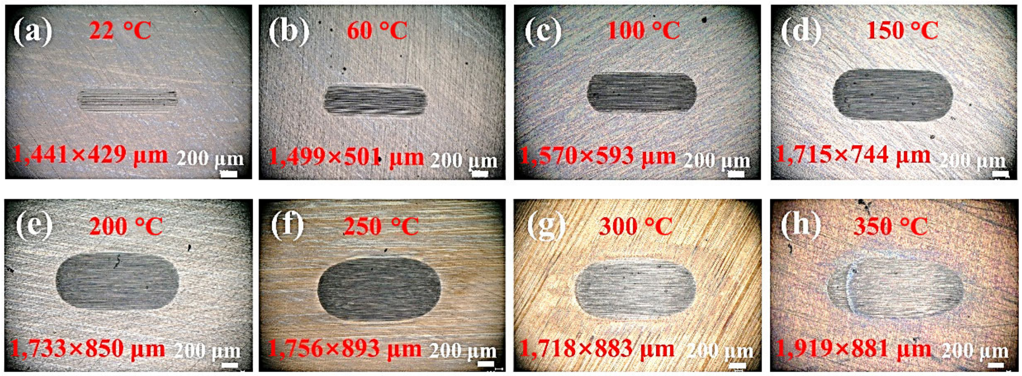

Fig. 5 Wear scar size of M50 steel discs at (a) 22 °C, (b) 60 °C (c) 100 °C, (d) 150 °C, (e) 200 °C, (f) 250 °C, (g) 300 °C, (h) 350 °C by 100× optical microscope.

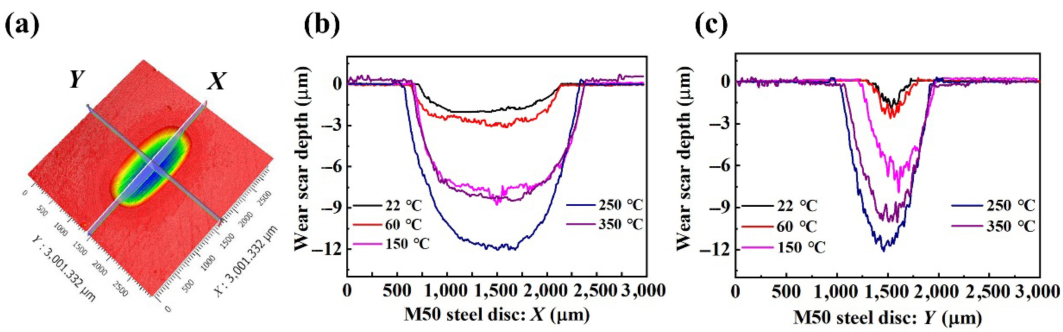

Fig. 6 (a) Topography of M50 steel discs, (b) *X* and (c) *Y* depth profiles of wear scar at different temperatures.

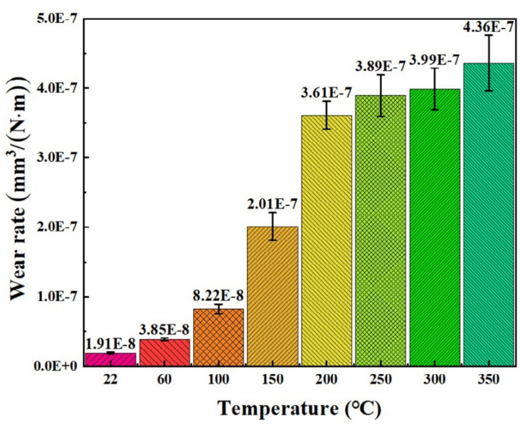

Fig. 7 Wear rate of M50 steel discs at different temperatures.

Even the wear rate of M50 steel disc under high temperature is still almost 2.2–22.8 times higher than those below 150 °C, the change in wear rate between high temperatures is only 20.7%. This means that the wear rate of M50 steel and Si_3N_4 ceramic barely changes when temperatures are above 150 °C. The inflection point at 150 °C is mainly caused by two reasons. One is the lubrication film formed between friction pairs. The other is the decreased contact pressure due to the enlarged WSS [34]. The results indicated that CPSO can provide long-term effective lubrication even when the temperature is up to 350 °C.

3.2 CPSO lubrication mechanism

In order to explore the change of chemical bonds and functional organic groups of CPSO before and after tribological tests, the used CPSO was collected and used for infrared spectral characterization and the fresh CPSO was used as the control sample. The CPSO shows stretching vibration absorption peaks of functional groups such as C–Cl (705 cm^{-1}), Ph-phenyl (1,400–1,600 cm^{-1}), Si–O–Si (1,060 cm^{-1}), Si–O (1,260 cm^{-1}), and Si–OH (3,628 cm^{-1}), as shown in Fig. 10 [35, 36]. The absorption peaks at 1,260, 1,060, and 809 cm^{-1} are significantly higher than those at 250 and 150 °C, which represent Si–O, Si–O–Si and $Si–CH_3$ bonds respectively. The oil after tribological tests shows an obviously wider absorption peak at 3,164 cm^{-1}, which is the vibration absorption peak of the –OH. Another wide absorption peak at 3,451 cm^{-1} appears, which is

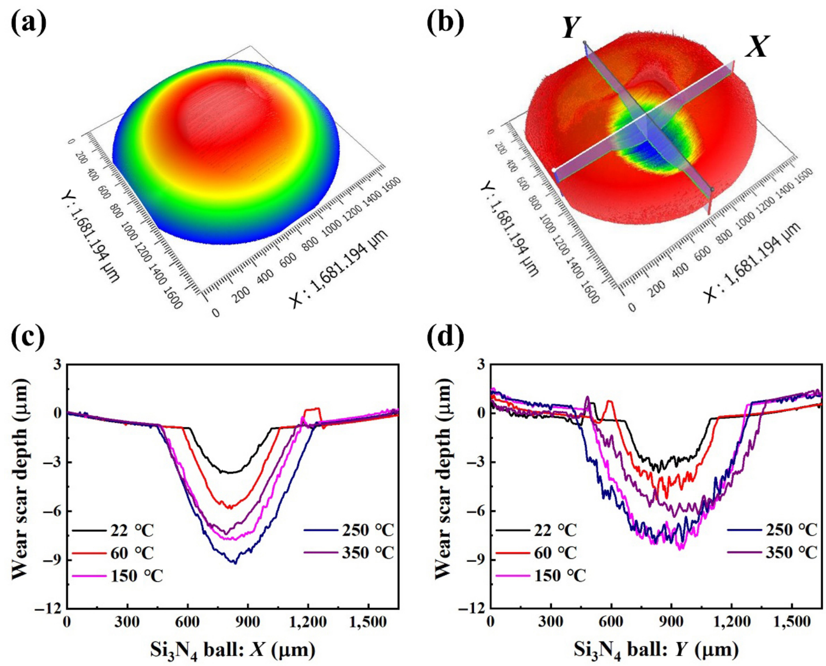

Fig. 8 (a) Surface topography of Si_3N_4 balls, (b) depth topography of Si_3N_4 balls, (c) *X* and (d) *Y* depth profiles of wear scar at different temperatures.

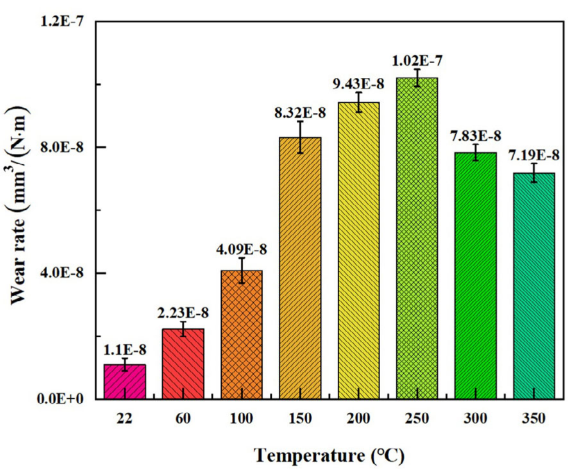

Fig. 9 Wear rate of Si_3N_4 balls at different temperatures.

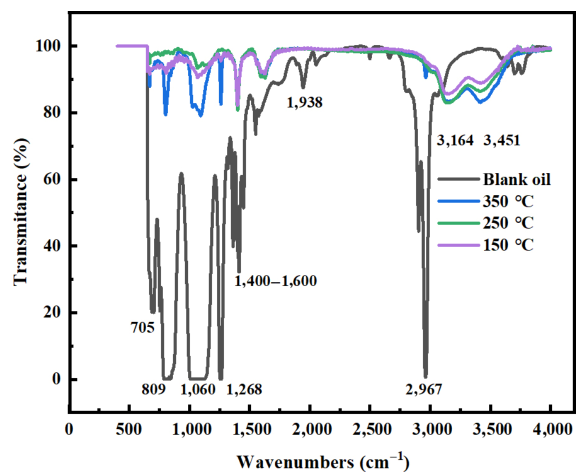

Fig. 10 Infrared spectra of fresh CPSO and CPSO after tribological tests at 350, 250, and 150 °C.

the vibration absorption peak of the intermolecular hydrogen bonding of –OH group [37]. The –OH group should be the methyl functional groups produced under high temperature during the abrasion such as methanol, formaldehyde, and formic acid [26]. It is likely that part of the CPSO functional groups have been oxidized to form other cracking products with the –OH group.

To reveal the effects of temperature on tribology performance of CPSO lubrication, the morphology of the worn surfaces was observed using SEM, as shown in Figs. 11(a)–11(d). The wear tracks lubricated by CPSO have characteristic grooves oriented parallel to the sliding direction observed. Differences in the furrow of worn surfaces could be seen when the temperature is different. Furrows on the surface of samples are neat and clean at 22 to 150 °C. There are almost no residuals on the surface. The obvious furrows and few abrasive particles indicating the occurrence of adhesive wear and abrasive wear during the friction process. When the temperature is above

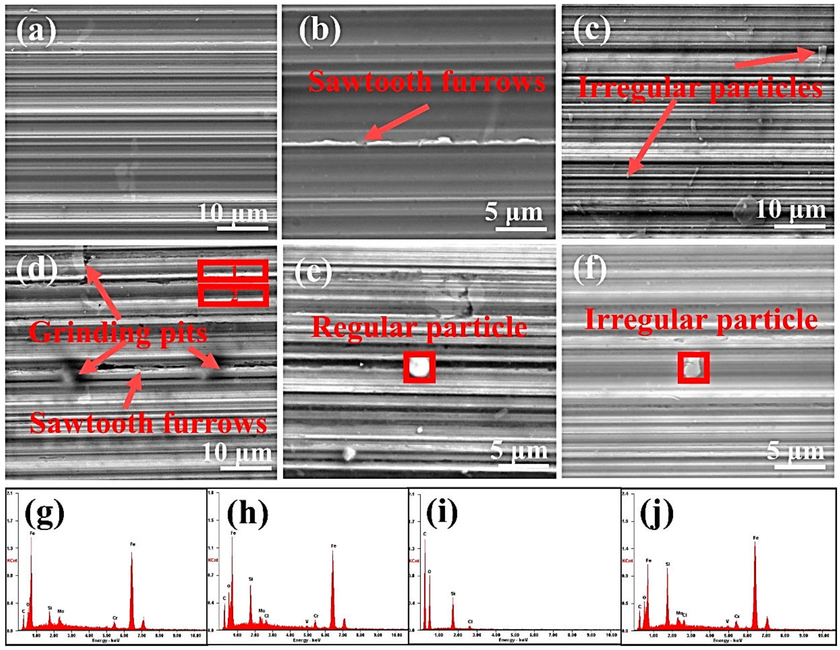

Fig. 11 SEM morphology results of M50 steel discs at different temperatures: (a) 60 °C, (b) 150 °C, (c) 250 °C, (d) 350 °C, (e) regular particles at 250 °C, (f) irregular particles at 250 °C, EDS results of (g) 1# area, (h) 2# area, (i) regular particle, (j) irregular particle.

150 °C, grinding pits, irregular particles and sawtooth furrows could be observed on the surface. When the temperature becomes even higher, a large amount of material is removed from the contact area and more severe abrasive wear occurs. This could explain the jitter of the COF curve.

The EDS results would be helpful to identify where these particles come from. The EDS results of Figs. 11(g)–11(j) show these particles and their elemental compositions on the wear scar surface lubricated by CPSO after 60 min. The element distribution of two rectangular areas marked 1 (surface) and 2 (bottom) in Figs. 11(g) and 11(h) show different Si content. The higher content of Si (6.07%) at the surface compared with Si (2.33%) at the bottom indicates the presence of CPSO is much more on the wear track bottom. The EDS results of regular particles in Fig. 11(i) are C (38.43%), Si (13.74%), Cl (2.31%), and O (45.47%), and no Fe had been detected. The EDS results of irregular particles in Fig. 11(j) show that the Fe content is as high as 76.5%. Based on the analysis above, it can be speculated that some regular-shaped particles in the wear scar are high-temperature cracking products of CPSO, while the irregular particles are M50 inorganic particles produced by corrosion or fracture.

SEM results indicate that the corrosive reactions with iron during the sliding process produce such a black substance, which might be ferric chloride. XPS analysis was used to further clarify the chemical states of the typical elements on wear scar surface lubricated by CPSO. Figure 12 shows the XPS spectra of Fe 2p, Cl 2p, and Si 2p on the worn surface of the discs. The Fe 2p peak at 711.2 and 710.2 eV can be identified as Fe_2O_3 and $FeCl_2$. The Cl 2p peak at 198.5 and 200.0 eV

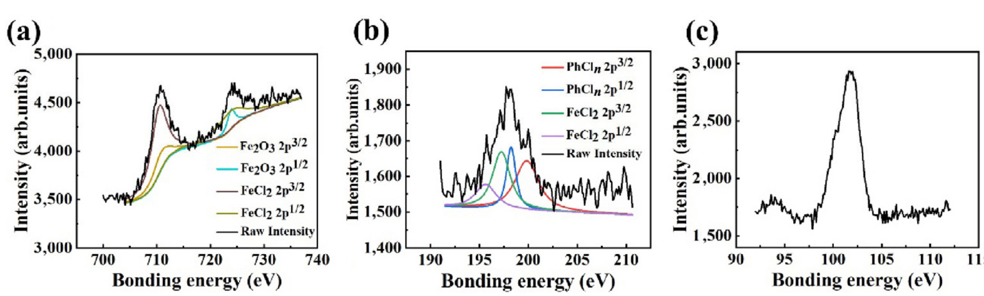

Fig. 12 XPS spectra at 350 °C of (a) Fe 2p, (b) Cl 2p and (c) Si 2p on worn surface of M50 steel discs.

can be identified as $FeCl_2$ and organic chlorine fragment of $–PhCl_n$ in CPSO. The peak of Si 2p appears at 102.4 eV, such binding energy belongs to $O–Si–(CH_3)_3$ of CPSO [22].

Together with the SEM and XPS results, it can be concluded that CPSO was firstly adsorbed on the surface of M50 steel disc and Si_3N_4 ball to form adsorption oil film. As the sliding process continues, the complex tribochemical reaction between CPSO adsorption film and M50 surface will occur to form the $FeCl_2$ film under the generated extreme pressure and heat. This tribochemical film prevents further wear.

According to the above analysis, the mechanism of tribological performance of Si_3N_4 ball on M50 steel disc lubricated by CPSO is illustrated in Fig. 13. In the beginning, CPSO molecules are adsorbed on the surface of Si_3N_4 ball on M50 steel disc to form the adsorption film [32]. When the temperature is below 150 °C, CPSO molecules shrink into a spring state. The boundary film is thick due to the relatively high viscosity. Clear furrows indicate that the wear mechanisms here are adhesive wear and abrasive wear, with adhesive wear dominated. As the temperature increases over 150 °C, CPSO molecules are stretched, which makes the viscosity of CPSO decrease. The wear between friction pair is more severe, the fracture of M50 generates inorganic irregular particles and the cracking of CPSO generates organic regular particles. With the increment of abrasive particles, the dominated mechanism changes from adhesive wear to abrasive wear. Furthermore, these two particles mentioned above will increase as the temperature change from 150 to 350 °C, which is helpful to the formation of $FeCl_2$ protective film. The thicker $FeCl_2$ film will further reduce the wear rate at high temperatures by improving wear resistance and load-bearing capacity. The lower contact pressure due to the increased WSS will also reduce the load on the boundary film. Therefore, the thicker $FeCl_2$ protective film and the reduced pressure within the contact region are main reasons for the decrease in the wear rate growth of M50 disc.

4 Conclusions

In this study, the tribological performance and lubrication mechanism of high-temperature liquid lubricant that can be used at 350 °C is reported for the first time. Results in this paper provide reliable supporting data for the construction of a M50-to-Si_3N_4 friction pair system using fluid CPSO lubricant for long-time and high-temperature service conditions.

The experimental temperature increases from 22 to 350 °C and CPSO exhibits interesting temperature-dependent lubrication law. Below 150 °C, COF remains

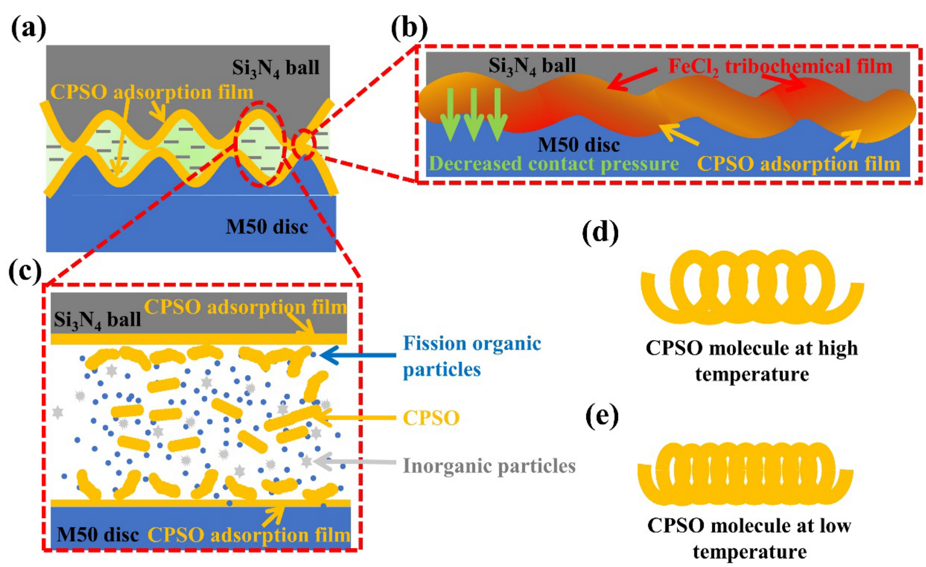

Fig. 13 Schematic diagrams of the tribology mechanism of CPSO: (a) overall schematic of Si_3N_4 ball and M50 steel disc, (b) microscopic schematic of contact area, (c) microscopic schematic of uncontacted area, (d) CPSO molecule at high temperature, and (e) CPSO molecule at low temperature.

stable at 0.13–0.15 after the initial running-in stage (600 s), while the COF in the running-in stage is in the range of 0.2–0.3. At 150 °C and above, the running-in time is much longer (1,200 s), and the instantaneous maximum value of COF can reach about 0.5. Under this condition, the COF gradually decreases and finally stabilizes at around 0.16–0.17 after the running-in stage. The different running-in period time is mainly due to the thickness of boundary adsorption film. The wear rate of M50 increases more than 954.9% at temperatures below 150 °C, while the wear rate growth slows down only about 20.7% at temperatures above 200 °C, indicating the as-built lubrication system has good anti-wear capability at high temperatures up to 350 °C.

The possible mechanistic explanation is that the complex tribochemical reactions between CPSO adsorption film and M50 surface will occur to form the $FeCl_2$ film. This protective film is generated on the metal surface to improve the anti-wear capacity. Irregular inorganic particles and regular organic particles generate more at the friction pair interface during the temperature increases from 150 to 350 °C, which contributes to the formation of $FeCl_2$ tribochemical reaction film. At high temperatures (200–350 °C), the anti-wear and load-bearing capacity of the boundary film has been improved, as the formed $FeCl_2$ productive film keeps getting thicker. The decreased pressure within the contact region will also reduce the load on the boundary film due to the increased WSS. As a result, the wear rate growth of M50 steel has an inflection point at 150 °C.

This main finding demonstrates that CPSO as a lubricant is capable of working under conditions at 350 °C, while most other lubricants will fail once the temperature exceeds 300 °C. Results in this paper provide a theoretical basis and data support for the high temperature lubricant and ceramic-to-steel friction pairs system.

Acknowledgements

This work was supported by the National Natural Science Foundation of China (Nos. 52275198, 52075037, 51805292), Fundamental Research Funds for the Central Universities (Nos. 2021XJJD01), Beijing Natural Science Foundation (No. 22C10149, 2202020) and Tribology Science Fund of State Key Laboratory of Tribology (Nos. SKLTKF21A01, SKLT2022B11).

Declaration of competing interest

The authors have no competing interests to declare that are relevant to the content of this article. The author Yonggang MENG is the Associate Editor of this journal. The author Yu TIAN is the Editorial Board Member of this journal.

References

[1] Meng Y G, Xu J, Jin Z M, Prakash B, Hu Y Z. A review of recent advances in tribology. *Friction* **8**(2): 221–300 (2020)

[2] Guan J. Research on rolling contact fatigue damage behavior of m50 bearing steel in aeroengine rolling bearing. Ph.D. Thesis. Harbin (China): Harbin Institute of Technology, 2019. (in Chinese)

[3] Tang, G Z, Xu, F J, Ma, X X. Microstructure and properties of surface modified layer for M50 steel by high current pulsed electron beam. *Heat Treat Met* **35**(7): 62–65 (2010) (in Chinese)

[4] Ge Q J, Zhang X H, Ma X X, Chen X G, Tang G Z. Tribological Properties of TiN Coated M50 Steel for High Temperature Bearing Against Sliver Coatings. *Aeronautical Manufacturing Technology* (**Z2**): 54–58 (2017) (in Chinese)

[5] Dante R C, Kajdas C K. A review and a fundamental theory of silicon nitride tribochemistry. *Wear* **288**: 27–38 (2012)

[6] Wang L, Snidle R W, Gu L. Rolling contact silicon nitride bearing technology: A review of recent research. *Wear* **246**(1–2): 159–173 (2000)

[7] Liu W M, Xu J, Feng D P, Wang X B. The research status and prospect of synthetic lubricating oils. *Tribology* **33**(1): 91–104 (2013) (in Chinese)

[8] Feng D P, Weng L J, Liu W M. Progress of tribology of perfluoropolyether oil. *Mocaxue Xuebao/tribology* **25**(6): 597–602 (2005)

[9] Wang D. Lubricating oil of future aviation engine. *Synthetic Lubricants* **32**(4): 26–29 (2005)

[10] Zhu L Y, Chen L G, Liu H C, Lei J, Zhang N S. Tribological and corrosion behaviors of benzotriazolium ionic liquids as lubricants of steel-steel system. *Tribology* **34**(6): 715–721 (2014) (in Chinese)

[11] Li H J, Tian P Y, Lu H Y, Jia W P, Du H D, Zhang X J, Li Q Y, Tian Y. State-of-the-art of extreme pressure lubrication realized with the high thermal diffusivity of liquid metal. *ACS Appl Mater Interfaces* **9**(6): 5638–5644 (2017)

[12] Bai P P, Li S W, Tao D S, Jia W P, Meng Y G, Tian Y. Tribological properties of liquid-metal galinstan as novel additive in lithium grease. *Tribol Int* **128**: 181–189 (2018)

[13] Bai P P, Li S W, Jia W P, Ma L R, Meng Y G, Tian Y. Environmental atmosphere effect on lubrication performance of gallium-based liquid metal. *Tribol Int* **141**: 105904 (2020)

[14] Andriot M, Chao S H, Colas A, Cray S, DeBuyl F, DeGroot J V, Dupont A, Easton T, Garaud J L, Gerlach E, et al. Chapter 2—Silicones in industrial applications. *Inorganic polymers*: 61–161 (2007)

[15] Ebert F J. Performance of silicon nitride (Si_3N_4) components in aerospace bearing applications. In Proceedings of the ASME 1990 International Gas Turbine and Aeroengine Congress and Exposition, Brussels, Belgium, 1990.

[16] Wang L, Wood R J K, Harvey T J, Morris S, Powrie H E G, Care I. Wear performance of oil lubricated silicon nitride sliding against various bearing steels. *Wear* **255**(1–6): 657–668 (2003)

[17] Shi H T, Bai X T. Model-based uneven loading condition monitoring of full ceramic ball bearings in starved lubrication. *Mechanical Systems and Signal Processing* **139**: 106583 (2020)

[18] Lin, G Y, Wang, S R, Wang, L P. Frictional performance and leakage of ball bearings lubricated by chlorphenyl silicone oil in vacuum. *Tribology* **29**(6): 526–530 (2009) (in Chinese)

[19] Weng L J, Wang H Z, Feng D P, Pan G M, Duan Y R, Liu W M, Xue Q J. Synthesis and tribological behavior of a chlorinated-phenyl methyl-terminated silicon oil as aerospace lubricant. *Mocaxue Xuebao/tribology* **25**(3): 254–257 (2005)

[20] Schiefer H M, Awe R W, Whipple C L. Extending the utility of silicone lubricants through structural modifications. *J Chem Eng Data* **6**(1): 155–160 (1961)

[21] Schiefer H M, Van Dyke J. Boundary lubricating properties of fluoroalkyl silicones in bench and pump tests. *S L E Trans* **7**(1): 32–42 (1964)

[22] Weng L J, Wang H Z, Feng D P, Liu W M, Xue Q J. Tribological behavior of the synthetic chlorine- and fluorine-containing silicon oil as aerospace lubricant. *Ind Lubr Tribol* **60**(5): 216–221 (2008)

[23] Jiang K J, Zhang X. Lubricity of fluorosilicone. *Journal of Aeronautical Materials* **31**(4): 81–85 (2011) (in Chinese)

[24] Lv M, Yang L J, Wang Q H, Wang T M, Liang Y M. Tribological performance and lubrication mechanism of solid–liquid lubricating materials in high-vacuum and irradiation environments. *Tribol Lett* **59**(1): 20 (2015)

[25] Munavirov B, Black J J, Shah F U, Leckner J, Rutland M W, Harper J B, Glavatskih S. The effect of anion architecture on the lubrication chemistry of phosphonium orthoborate ionic liquids. *Sci Rep* **11**: 24021 (2021)

[26] Wu Q. Silicone oil and lubricate. *Journal of Shaanxi Normal University (Natural Science Edition)* **(Z01)**: 163–172 (1981) (in Chinese)

[27] Zhou N. *Introduction of silicone polymer*. Beijing: Science Press, 2000.

[28] Dube M J, Bollea D, Jones W R, Marchetti M, Jansen M J. A new synthetic hydrocarbon liquid lubricant for space applications. *Tribol Lett* **15**(1): 3–8 (2003)

[29] Li X, Lin F J, Du S M, Wu C C. Comparative analysis of high performance bearing steels. *Heat Treatment of Metals* **46**(6): 14–20 (2021) (in Chinese)

[30] Khonsari M M, Ghatrehsamani S, Akbarzadeh S. On the running-in nature of metallic tribo-components: A review. *Wear* **474–475**: 203871 (2021)

[31] Blau P J. On the nature of running-in. *Tribol Int* **38**(11–12): 1007–1012 (2005)

[32] Wen X L, Bai P P, Meng Y G, Ma L R, Tian Y. High-temperature superlubricity realized with chlorinated-phenyl and methyl-terminated silicone oil and hydrogen-ion running-in. *Langmuir* **38**(32): 10043–10051 (2022)

[33] Zhang C W, Peng B, Wang L Q, Ma X X, Gu L. Thermal-induced surface damage of M50 steel at rolling-sliding contacts. *Wear* **420–421**: 116–122 (2019)

[34] Aisyah I S, Caesarendra W, Kurniawati D, Maftuchah M, Agung D, Glowacz A, Oprzędkiewicz K, Liu H. Study of jatropha curcas linn and olea europaea as bio-oil lubricant

to physical properties and wear rate. *Lubricants* **9**(4): 39 (2021)

[35] Peng H L, You X Z, Xu X M, Qiu B L, Shao Y G. Synthesis Process of Methylphenyl Silicone Resin. *Insulating Materials* **44**(4): 16–19 (2011) (in Chinese)

[36] Li C X. Infrared spectroscopeic analysis of synthetic lubes. *Synthetic Lubricants* **42**(4): 36–40 (2015) (in Chinese)

[37] Freedman H H. Intramolecular H-bonds. I. A spectroscopic study of the hydrogen bond between hydroxyl and nitrogen. *J Am Chem Soc* **83**(13): 2900–2905 (1961)

Yan MENG. He is now a Ph.D. candidate in the School of Mechanical and Electrical Engineering, China University of Mining and Technology-Beijing. His current research focuses on the high temperature lubrication of the bearing steel.

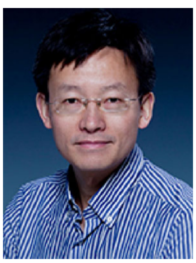

Yu TIAN. He is professor and director of the State Key Laboratory of Tribology in Advanced Equipment at Tsinghua University, China. He gained his B.S. and Ph.D. degrees in mechanical engineering at Tsinghua University in 1998 and 2002, respectively. He was a postdoc at the University of California, Santa Barbara, USA, with Professor Jacob ISRAELACHVILI from 2005 to 2007. He has published over 200 peer-reviewed journal papers. He has received the Ten Thousand People Leading Plan Innovation Leading Talents of China (2019), the Youth Science and Technology Award of China (2016), the Yangtze River Scholars Distinguished Professor (2015–2019), the National Science Found for Distinguished Young Scholars of China (2014), the Wen Shizhu-Maple Award-Young Scholar Award (2012), the Young Scholar Achievement Award of the Society of Mechanical Engineering of China (2011), the Outstanding Young Scholar Award of the Chinese Tribology Institute (2009), and the National Excellent Doctoral Dissertation of China (2004). His research interest is the science and technology at the interface of physics, materials, engineering, and biology to understand the physical laws of adhesion, friction, and rheology to implement technological inventions to benefit the society.

Jie CHENG. She is professor in the School of Mechanical and Electrical Engineering, China University of Mining and Technology-Beijing. She obtained her Ph.D. from Tsinghua University, China, in 2016 and B.E. from Shandong University, China, in 2011, and worked as a postdoctoral fellow at Tsinghua University and KTH Royal Institute of Technology, Sweden, during 2017–2019. She received the Young Elite Scientists Sponsorship Program by China Association for Science and Technology (CAST; 2022). Her current research interests emphasize the use of corrosion science, tribology technology, and surface & interface techniques to: 1) study the chemical mechanical polishing (CMP) technology of integrated circuit fabrication for advanced technology node; 2) develop bio-inspired green multifunctional coatings for engineering purpose; 3) ultra-precision machining of photovoltaic cell panel to increase the power generation efficiency.